



Carotenoid responds to excess energy dissipation in the LH2 complex from *Rhodoblastus acidophilus*

Ivana Šímová¹ · Valentyna Kuznetsova¹ · Alastair T. Gardiner² · Václav Šebelík^{1,3} · Michal Koblížek² · Marcel Fuciman¹ · Tomáš Polívka¹

Received: 22 June 2022 / Accepted: 17 August 2022 / Published online: 6 September 2022
© The Author(s), under exclusive licence to Springer Nature B.V. 2022

Abstract

The functions of both (bacterio) chlorophylls and carotenoids in light-harvesting complexes have been extensively studied during the past decade, yet, the involvement of BChl *a* high-energy Soret band in the cascade of light-harvesting processes still remains a relatively unexplored topic. Here, we present transient absorption data recorded after excitation of the Soret band in the LH2 complex from *Rhodoblastus acidophilus*. Comparison of obtained data to those recorded after excitation of rhodopin glucoside and B800 BChl *a* suggests that no Soret-to-Car energy transfer pathway is active in LH2 complex. Furthermore, a spectrally rich pattern observed in the spectral region of rhodopin glucoside ground state bleaching (420–550 nm) has been assigned to an electrochromic shift. The results of global fitting analysis demonstrate two more features. A 6 ps component obtained exclusively after excitation of the Soret band has been assigned to the response of rhodopin glucoside to excess energy dissipation in LH2. Another time component, ~450 ps, appearing independently of the excitation wavelength was assigned to BChl *a*-to-Car triplet–triplet transfer. Presented data demonstrate several new features of LH2 complex and its behavior following the excitation of the Soret band.

Keywords Carotenoids · Antenna complex · LH2 · Energy transfer · Excess energy · Electrochromic shift

Introduction

Life on Earth depends on utilization of solar radiation as the primary source of energy. Photosynthetic organisms contain light-harvesting complexes incorporating intricate pigment-protein systems that efficiently absorb solar radiation. Light-harvesting complexes exhibit large variation across the variety of photosynthetic organisms, reflecting the light conditions of the environment in which they live. Photon capture is achieved via photosynthetic pigments,

(Bacterio) chlorophylls (B) (Chl), carotenoids, and bilins, which have their absorption bands tuned to absorb sunlight and transfer excitation energy within and between pigment-protein complexes to the reaction centers where charge separation occurs (Blankenship 2008). The development of time-resolved spectroscopic techniques in the past two decades has significantly expanded our knowledge of excitation energy transfer in photosynthesis.

Many antenna proteins have been studied by ultrafast spectroscopy providing details about inter-pigment as well as inter-complex energy transfer processes (Croce and Van Amerongen 2014; Mirkovic et al. 2017; Polívka and Frank 2010). Nearly all these studies initiate the light-driven processes in antenna complexes by exciting the lowest-absorbing states of pigments; the Q_y states of (B) Chl or the S_2 state of carotenoids whose lowest energy state, S_1 , is forbidden for one-photon absorption (Polívka and Sundström 2004). Such an arrangement is suitable for following energy transfer between pigments or between complexes because processes related to the relaxation dynamics of the upper states do not interfere with the primary process of interest, inter-pigment or inter-complex energy transfer. On the other hand,

✉ Tomáš Polívka
tpolivka@jcu.cz

¹ Department of Physics, Faculty of Science, University of South Bohemia, Branišovská, 1760, 370 05 Ceske Budejovice, Czech Republic

² Laboratory of Anoxygenic Phototrophs, Institute of Microbiology, Czech Academy of Sciences, 379 81 Třeboň, Czech Republic

³ Dynamical Spectroscopy, Department of Chemistry, Technical University of Munich, Lichtenbergstraße 4, 85748 Garching b. Munich, Germany

the absorption maxima of upper excited states, such as the Soret or Q_x bands of (B) Chl, are still within the spectral profile of solar radiation reaching the Earth surface. Thus, they contribute to light harvesting, but our knowledge of how the excess energy excitation may affect this process is limited.

Steady-state fluorescence excitation spectra measured over the large span of excitation wavelengths showed that, expectedly, the energy absorbed by the Soret or Q_x bands of (B) Chls reaches the lowest Q_y state via internal conversion (Kosumi et al. 2013; Kosumi et al. 2011a). The dynamics of Soret relaxation has been studied for photosynthetic pigments only for Chl *a* and Chl *b* in solution, yielding the Soret lifetimes around 150 fs (Bricker et al. 2015; Shi et al. 2005). Comparable lifetimes were reported for Soret excitation of heme in myoglobin (Kholodenko et al. 2000). In light-harvesting complexes, the relaxation dynamics of upper excited states is limited to a few studies addressing the $Q_x - Q_y$ internal conversion. In the purple bacterial antenna, a 50 fs $Q_x - Q_y$ relaxation time was reported in the light-harvesting 2 (LH2) complex (Kosumi et al. 2011b), while the 100–200 fs Q_x relaxation was identified in LH1 (Visser et al. 1995). An even longer relaxation time of 200–300 fs was extracted from global fitting the data obtained after excitation of Chl *b* at 490 nm in the LHCII complex from higher plants (Croce et al. 2001).

Apart from relaxation dynamics of the upper excited states, an interesting question is whether the excess energy, which must be either stored in vibrations of the absorbing molecule itself or dissipated to the nearest environment (Balevičius et al. 2019), somehow affects the overall dynamical behavior of the system. Though never reported for light-harvesting proteins, propagation of disturbance through protein after excess energy excitation, sometimes termed as a ‘proteinquake’, has been experimentally demonstrated for cytochrome *c* (Zang et al. 2009) or myoglobin (Ferrante et al. 2016; Levantino et al. 2015). These results suggest that dissipation of excess energy, absorbed by a molecule after excitation of the upper energy states, may trigger processes inaccessible if the lowest energy states of the pigments are excited. For example, a light-driven cascade photoconversion of the orange carotenoid protein (Konold et al. 2019) utilizes the enigmatic S^* state of carotenoids, which is at least partly related to excess energy dissipation (Balevičius et al. 2016).

We have chosen the *Rhodoblastus (Rbl.) acidophilus* LH2 antenna complex as a model system to study the possible effects of excess energy dissipation after excitation of the Soret band of BChl *a*. The high-resolution structure of this complex is well known (McDermott et al. 1995) and energy transfer pathways within this complex have been extensively studied both after carotenoid (Cong et al. 2008; Magdaong et al. 2014) and BChl *a* excitation (Sundström et al. 1999), making the LH2 an ideal model

complex. Furthermore, the BChl *a* Soret band in LH2 peaks around 380 nm, allowing selective excitation without exciting the carotenoid rhodopin glucoside (absorption maximum at 490 nm) or tryptophan (280 nm). Despite the large amount of experimental and theoretical data obtained for the LH2 complex, there are still gaps in our knowledge. One of the unknowns is the relaxation dynamics after excitation of the Soret band. More than two decades ago, the possibility of energy transfer from BChl *a* Soret to the carotenoid S_2 state in LH2 was predicted (Tretiak et al. 2000), but later experiments using steady-state fluorescence excitation spectra did not reveal any evidence for such an energy transfer channel (Razjivin et al. 2021, 2017). Another energy transfer channel related to upper excited states was proposed by Kosumi et al. (2011b) who detected energy transfer from the Q_x state of BChl *a* to the S_1 state of the long carotenoid spirilloxanthin in LH1.

Another interesting, though not consistently explained, feature of LH2 is the presence of the carotenoid S^* signal. It was first identified in the LH1 complex of *Rhodospirillum (Rsp.) rubrum* (Gradinaru et al. 2001), and subsequently detected also in LH2, where it was associated with a separate excited state that even served as a minor energy donor in carotenoid-BChl *a* energy transfer (Papagiannakis et al. 2002). Later, unexpected dependence of the S^* signal in LH2 on excitation intensity (Papagiannakis et al. 2006) suggested a complicated involvement of S^* in the LH2 excited state processes (Jailaubekov et al. 2010). The intensity dependence of the S^* signal has never been reported for carotenoids in solution, where it was instead suggested to be related to energy dissipation channel (Balevičius et al. 2019; Lenzer et al. 2010), leading to a concept of different origins of the S^* signal in solution and in LH2. The last twist in the S^* story in LH2 was reported in 2016 (Niedzwiedzki et al. 2016), when analysis of transient absorption data assigned the S^* signal in LH2 to a phenomenon known from earlier experiments, the electrochromic shift of the carotenoid S_2 state upon excitation of BChl *a* in LH2 (Herek et al. 1998, 2004).

To resolve questions related to the role of upper excited states in LH2 excited state dynamics as well as the origin of the S^* signal, the magnitude of which is related to excess energy excitation (Billsten et al. 2005; Khan et al. 2021), we recorded transient absorption spectra in the 420–1100 nm spectral region after excitation of the Soret band of BChl *a* in LH2. Comparing these data with datasets obtained after carotenoid and B800 excitation we show there is no energy transfer between the BChl *a* Soret and carotenoid S_2 state. However, the Soret excitation generates a clear carotenoid electrochromic shift whose amplitude depends on whether the Soret or B800 band in LH2 is excited.

Materials and methods

Sample preparation

Cells of *Rbl. acidophilus* strain 10050 were grown anaerobically in C-succinate media at 30 °C under anaerobic conditions at a light intensity of $\sim 100 \mu\text{mol photons s}^{-1} \text{ m}^{-2}$. The fully grown culture was pelleted, washed once with 20 mM MES, 100 mM KCl, pH 6.8 to remove media traces and the cell pellet either used immediately or flash frozen until required. The *Rbl. acidophilus* cells were re-suspended in 20 mM Tris.Cl pH 8.0, homogenized thoroughly with a few grains of DNase and a few mg of MgCl_2 . The cells were broken by passage three times through an Emulsiflex-CS cell disrupter and the sample immediately placed in an ultracentrifuge (180,000 $\times g$, 90 min, 4 °C). The supernatant was discarded and the pelleted membranes gently re-suspended with 20 mM Tris.Cl pH 8.0 and adjusted to an optical density (OD) at the Q_x maxima (approx. 580 nm) of 50 cm^{-1} . The membrane suspension was solubilized at room temperature for 1 h with 1% *N, N*-dimethyldodecylamine *N*-oxide (LDAO) and then centrifuged to remove any un-solubilized material. The solubilized, supernatant fraction was fractionated using stepwise sucrose density centrifugation (150,000 $\times g$, 4 °C, 16 h). The LH2 complex band was gently removed from the gradient, loaded on an anion-exchange gravity column with ToyoPearl 650S resin (Tosoh) and eluted with increasing concentrations of NaCl in TL buffer (20 mM Tris.Cl, 0.1% LDAO, pH 8.0). The resulting fractions were assayed spectrophotometrically for purity and the best pooled, concentrated and run on a Sephacryl S-300 (GE Healthcare) size-exclusion column. The best fractions ($\text{Abs}_{.858 \text{ nm}}/\text{Abs}_{.275 \text{ nm}} \leq 3.2$) were pooled, concentrated and then flash frozen until required.

Spectroscopy

The transient absorption measurements have been performed on an experimental setup that consists of a femtosecond amplified system (Spectra Physics; MaiTai, Empower, and Spitfire Ace) that produces 800 nm ~ 100 fs laser pulses at 1 kHz. The system output is split into two beamlines: one seeds optical parametric amplifier TOPAS Prime that is tuned to different excitation wavelengths described in the main text; the second pulse seeds a home-built non-collinear optical parametric amplifier that is tuned to produce 1300 nm pulses. The 1300 nm beam is sent through the constantly moving non-linear CaF_2 crystal to generate white light supercontinuum in a broad spectral range spanning from 420 to 1100 nm. The

white light beam is divided into probe and reference with the sample positioned near its focal plane. The probe beam overlaps with the excitation beam (pump) at the sample position. The probe and reference beams are collimated, sent to a prism spectrograph designed to measure spectra in the full 420–1100 nm range with ~ 5 nm spectral resolution, and detected by a double-CCD array detector (Pascher Instruments, Sweden). The detection spectrometer was calibrated by a set of color filters (pre-measurement) and by a multiple oxide filter (post-measurement). The mutual polarization of pump and probe was set to magic angle (54.7°). The computer-controlled delay line in the probe pulse is used to set time delays up to 6 ns between the pump and the probe. The sample is placed in the 2 mm quartz cuvette with a magnetic stirrer at room temperature. The excitation photon density was maintained around 3.4×10^{13} and $7 \times 10^{13} \text{ photons.cm}^{-2}.\text{pulse}^{-1}$ for 380 nm and 800 nm, respectively. The sample absorption spectra were measured before and after transient absorption experiments to ensure that the samples did not degrade during the experiment.

Data analysis

The spectrally calibrated datasets were analyzed using commercial software (CarpetView, Light Conversion, Lithuania). For the global analysis, sequential irreversible evolution scheme was considered whose resultant spectral profiles are called evolution-associated difference spectra (EADS). Prior to global analysis, all data were proceeded by background subtraction and chirp correction. To simulate the kinetic of the triplet rise, a simple Python script was developed. It uses a set of differential equations, which describe the time-dependent populations of individual species, solved by the Euler method and applies these to the species of interest to obtain the simulated kinetics.

Results

Steady-state absorption

Steady-state absorption spectrum of the LH2 antenna complex from *Rbl. acidophilus* strain 10050 is given in Fig. 1. The spectral features are assigned to the electronic transitions of BChl *a*: Soret band at ~ 380 nm, Q_x band at 580 nm, and two Q_y bands at 800 (B800) and 860 nm (B850). The characteristic three-peak structure around 420–500 nm corresponds to the absorption bands of the S_2 excited state of the carotenoid rhodopin glucoside. The vertical arrows indicate the excitation wavelengths used in the current study. The Soret band has been excited to the maximum at 380 nm as well as to the higher energy shoulder at 360 nm and 340 nm

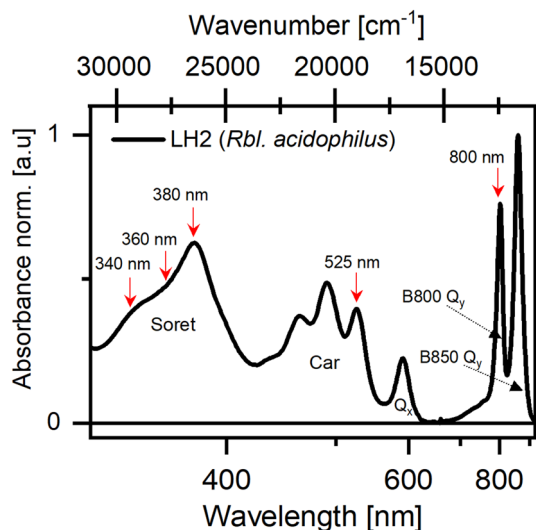


Fig. 1 Absorption spectrum of LH2 complex from *Rbl. acidophilus*. The red arrows represent excitation wavelengths used in the transient absorption experiments

to provide even higher excess energy excitation and to eliminate possible excitation of the high energy tail of rhodopin glucoside absorption. Rhodopin glucoside was excited at the maximum of the 0–0 band of the S_0 – S_2 transition at 525 nm to avoid any relaxation processes within the carotenoid S_2 state. To provide reference data for the Soret excitation, we have also excited the B800 band.

Excited state dynamics

Transient absorption spectra measured after different excitations are shown in Fig. 2. Although the spectra have been measured in the full 420–1100 nm spectral range in a single experiment, for the sake of clarity, we present the transient absorption spectra split into two parts. This is done because the amplitude of transient BChl a bands in the near-IR region is about order of magnitude larger than the signal amplitude in the 420–700 nm region (note different vertical axis scales in the panels showing the visible and near-IR spectral regions).

Excitation of the Soret band at 380 nm (see Supporting Information, Fig. S1 for other excitation wavelengths within the Soret band) generates characteristic transient pattern in the 800–950 nm spectral region (Fig. 2B) consisting of overlapping excited state absorption and ground state bleaching/stimulated emission bands originating predominantly from the B850 BChl a . The transient absorption spectrum at 0.2 ps after excitation contains a clear negative band at 800 nm, indicating that B800 BChl a is also excited at 380 nm. The contribution of the B800 bleaching is even more distinguished for 340 and 360 nm excitations (Supporting Information, Fig. S2). The B800 bleaching

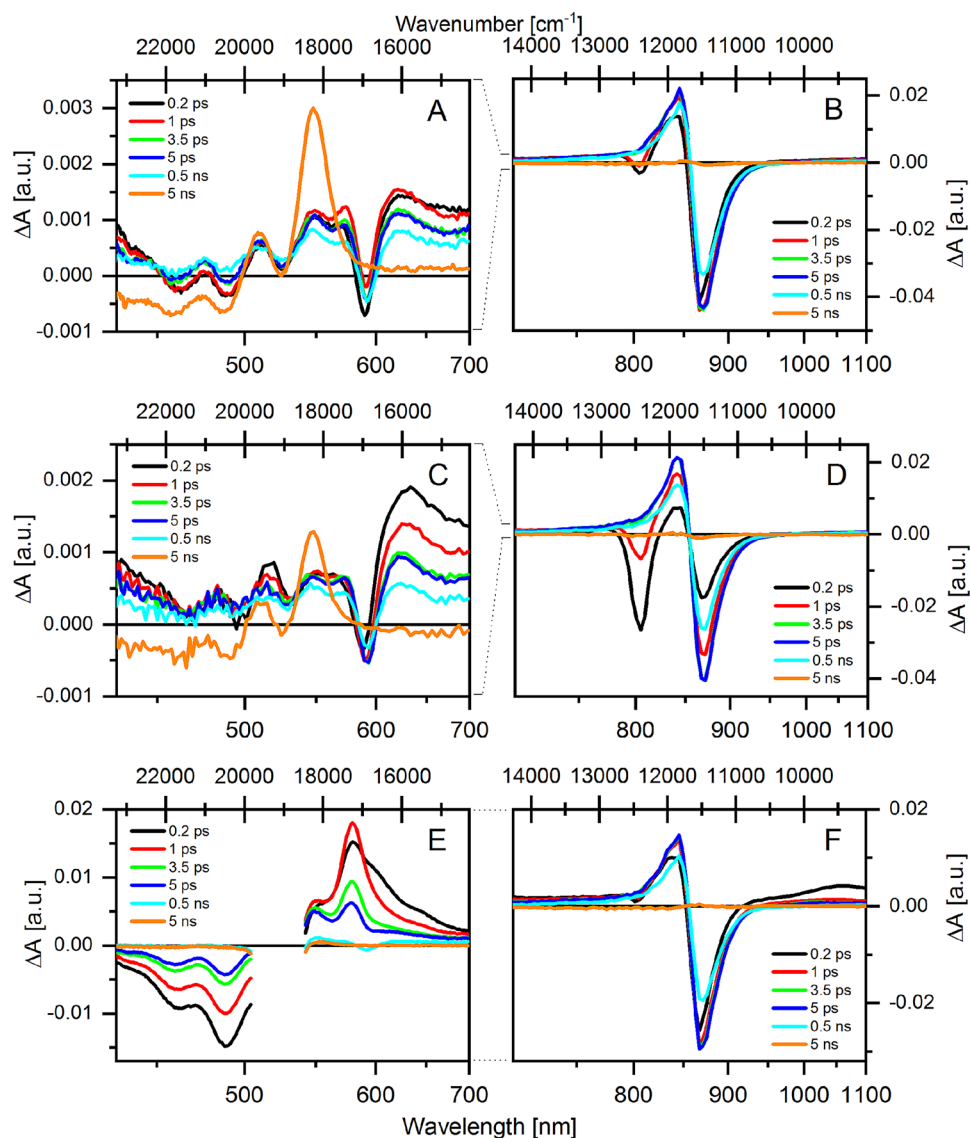
disappears within first few picoseconds, reflecting the known B800–B850 energy transfer dynamics in LH2 (Kennis et al. 1997; Ma et al. 1997).

The 420–700 nm spectral region (Fig. 2A) shows weaker in magnitude, but richer in structure signal. The central feature of the 0.2 ps spectrum is bleaching of the BChl a Q_x band at 590 nm that is accompanied by excited state absorption in the 600–700 nm region. The dynamics of this signal indicates origin from BChl a . The spectral region of carotenoid ground state absorption exhibits clear signal, reminiscent of the pattern earlier identified as due to electrochromic shift (Herek et al. 1998; Niedzwiedzki et al. 2016). This signal has complex dynamics as the first decay takes place within the first few hundreds of picoseconds (the band amplitudes are significantly diminished in 500 ps spectrum), but at later times the bleaching bands gain amplitude again due to formation of the carotenoid triplet state. The characteristic triplet spectrum with maximum at 550 nm is the dominant feature of the 5 ns spectrum, which contains almost no BChl a contribution signaling efficient BChl a –Car triplet–triplet energy transfer.

Data obtained after 800 nm excitation (Fig. 2C, D) produces less pronounced bands in the carotenoid region, but the overall pattern is qualitatively similar to the Soret excitation except the B800 bleaching in the near-IR region that is obviously much more pronounced than after the Soret excitation. The appearance of signal in the carotenoid region confirms the signal assignment to the carotenoid electrochromic shift, because after Q_y band excitation there could not be any carotenoid population at timescales shorter than 500 ps. The B800 excitation further helps to identify the excited state absorption in the 600–700 nm region; this signal is strongest in the early (< 1 ps) spectra, implying it has significant contribution from B800 BChl a that decays within the first few picoseconds due to B800–B850 energy transfer.

To better assess the carotenoid signals obtained after Soret excitation, we have also carried out measurements after direct carotenoid excitation to the S_2 state (Fig. 2E, F). The visible part of the spectrum is now dominated by the carotenoid signals, ground state bleaching in the 420–510 nm region and S_1 – S_n excited state absorption in the 530–700 nm region. The excited state absorption band peaks at 580 nm with a distinct shoulder at 550 nm, which is more pronounced at longer delays showing difference in their relaxation dynamics. This shoulder is the S^* signal. Evolution of the spectra during the first picosecond corresponds to the vibrational cooling of the ‘hot’ S_1 state that evolves into the typical relaxed S_1 – S_n spectrum (green). In the near-IR, the early time spectra contain the carotenoid contribution due to a broad S_2 – S_N excited state absorption peaking around 1050 nm. There is also weak B800 bleaching in the early time spectra indicating the presence of carotenoid–B800 energy transfer via the S_2 pathway.

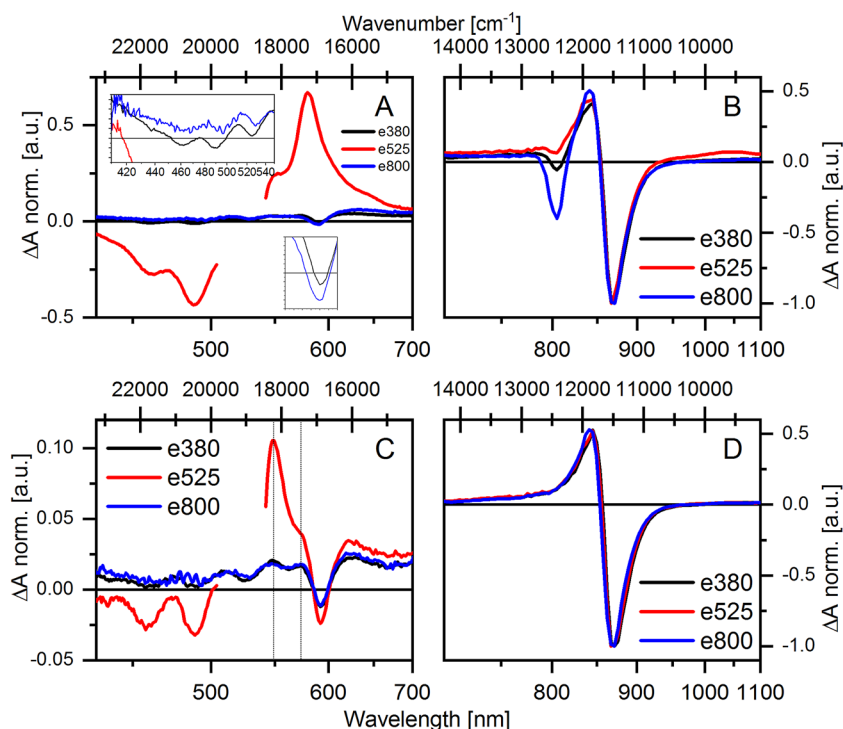
Fig. 2 Representative transient absorption spectra of LH2 from *Rbl. acidophilus* recorded after 380 nm (A, B), 800 nm (C, D), and 525 nm (E, F) excitation



The key differences between data obtained after excitation to the Soret, B800, and carotenoid S_2 state are highlighted in Fig. 3, which shows transient absorption spectra normalized to B850 bleaching at 0.5 (Fig. 3A, B) and 20 ps (Fig. 3C, D) delay times. In the near-IR spectral region, the 0.5 ps spectra demonstrate that B800 BChl a molecules are populated after both Soret and carotenoid excitation. At 20 ps, however, the normalized spectra are essentially identical showing that the final singlet excited state of BChl a , B850, is the same regardless the excitation wavelength. The differences in the visible spectral regions are dominated by the presence of strong carotenoid signals generated by carotenoid excitation, but further differences are identified when comparing the Soret and B800 excitations. First, at 0.5 ps there is a slight difference in positions of Q_x bleaching. We know that Soret excitation hits both B800 and B850

BChl a (Fig. 2B), thus the small blue shift of Q_x bleaching after B800 excitations implies that the blue part of the Q_x band is dominated by the B800 BChl a while the red part is due to B850 BChl a . At 20 ps, the Q_x positions are identical, further confirming the identity of the final state. The relative amplitude of the signal in the carotenoid region is for BChl a excitation slightly larger after Soret excitation at both 0.5 and 20 ps. Yet, for carotenoid excitation this amplitude is much larger (Fig. 3A, C). It is important to note that the data shown in Fig. 3 are normalized to B850 bleaching, thus the carotenoid signal should correspond to the same amount of excited B850. The relaxation dynamics of BChl a populated via energy transfer from carotenoid versus direct excitation of BChl a however leads to a markedly different magnitude of the carotenoid signal.

Fig. 3 Comparison of transient absorption spectra after 380 nm (black), 525 nm (red), and 800 nm (blue) excitation taken at 0.5 ps (**A, B**) and 20 ps (**C, D**). All spectra were normalized to the B850 ground state bleaching



Global analysis

We have applied a global analysis to get better insight into the dynamics of the system as well as to estimate involvement of different excited states in relaxation processes. Given the complexity of the system and the fact that the richer dynamics occurs in a spectral region where the signal amplitude is small compared to the main spectral bands in the near-IR, we have fitted the near-IR (700–1100 nm) and visible (420–700 nm) spectral region separately. We first fitted the near-IR region that is dominated by BChl *a* signals and thus represents nearly pure BChl *a* dynamics. The near-IR spectral region was fitted by the minimal number of components required to obtain a reasonable fit and the obtained time constants were used as initial values for fitting the visible spectral region. All data were initially fitted to a sequential model resulting in evolution-associated difference spectra (EADS) and results are shown in Fig. 4.

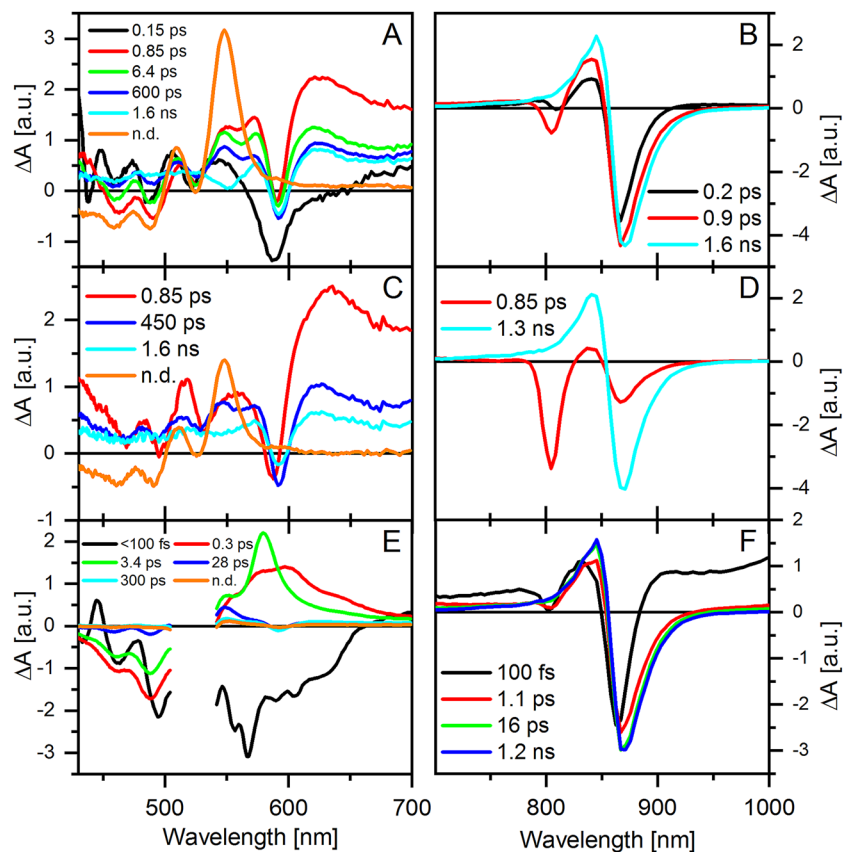
We will begin the description of global fitting results with data obtained after B800 excitation, which require the lowest number of components. In the near-IR spectral region (Fig. 4D), only two components are needed. The initially excited state has distinct B800 bleaching signal, but also a contribution from B850 resulting in excitation of upper excitonic band of B850, too (Koolhaas et al. 1998). This state decays with 0.85 ps time constant to form the characteristic B850 signal, thus reflecting the well-known B800-to-B850 energy transfer. The B850 decays within 1.3 ns corresponding to the known lifetime of free LH2. No other components

are needed to fit the data, confirming that we work in an annihilation-free regime. Moving to the visible spectral region (Fig. 4C), the similar time constants appear in the fit, 0.85 ps and 1.6 ns. The spectral profile of the 0.85 ps component (red) shows that B800 BChl *a* significantly contributes to the excited state absorption in the 600–700 nm spectral region as well as at the wavelengths below 450 nm. Yet, one extra component, 450 ps (blue), is needed to fit the data. This component is crucial to fit the data in the spectral region of the carotenoid triplet, which peaks at 550 nm as evidenced from the final, non-decaying EADS (orange) that represents the pure carotenoid triplet. Without this component, the triplet kinetics cannot be fitted (see Supporting Information, Fig. S3 to see the fit without the 450 ps component). Since no such component is needed to fit the BChl *a* signal in the near-IR, it must be related to the carotenoid dynamics.

For the Soret excitation, the EADS extracted from fitting the near-IR region (Fig. 4B) are comparable to those obtained after B800 excitation, but an additional fast (0.2 ps) component is needed. Here, the initial EADS (black) contains both B800 and B850 bleaching as both are excited at 380 nm. The fast, 0.2 ps process is associated with an increase of ESA around 830 nm and stimulated emission around 900 nm, indicating that the 0.2 ps process is due to relaxation from the Soret band to Q_y of both B800 and B850. The two other components, 0.9 ps and 1.6 ns, are due to the same processes as those described for B800 excitation.

The fit of the 420–700 nm spectral region (Fig. 4A) again gives the comparable components to those obtained from

Fig. 4 EADS obtained from the global fitting analysis after 380 nm (A, B), 800 nm (C, D), and 525 nm (E, F) excitation



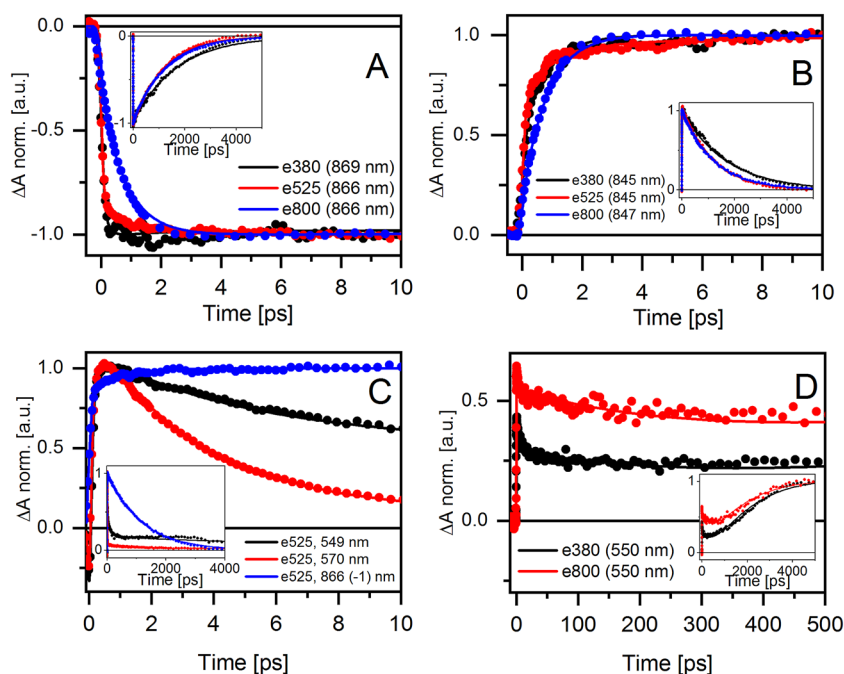
fitting the near-IR, 0.15 ps, 0.85 ps, and 1.6 ns, but for the Soret excitation two additional components are required to obtain reasonable fits. The initial component confirms the assignment to Soret-to- Q_y relaxation as it lacks the ESA signal in the 600–700 nm, which has been identified as due to B800 and B850 ESA (see above). Interestingly, however, already this initial EADS contains the wavy signal in the carotenoid region, again pointing to its origin as due to electrochromic shift resulting from response of carotenoid to excited BChl *a*. The 0.85 ps (red) and 1.6 ns (cyan) components are due to B800 and B850 and associated dynamics reflects the B800-to-B850 energy transfer and B850 decay, respectively. As for the B800 excitation, EADS having a time constant of a few hundreds of picoseconds (600 ps here, blue EADS), is needed to fit the triplet kinetics around 550 nm. However, one extra EADS (green) characterized by the 6.4 ps time constant is needed to fit the carotenoid region after Soret excitation. Its spectral profile indicates that it is associated with a decrease of amplitude of the wavy signal in the carotenoid region, but it also has a non-negligible amplitude in the 600–700 nm region where ESA of B850 is expected.

Finally, the EADS obtained from data after carotenoid excitation match those reported for this LH2 complex earlier (Cong et al. 2008). In the near-IR (Fig. 4F), the initial EADS (black) contains signals from both B800 and B850 bleaching

as well as the ESA signal from carotenoid S_2 state, confirming the sub-100 fs energy transfer from the carotenoid S_2 state to both B800 and B850 (Macpherson et al. 2001). The second EADS (1.1 ps, red) still contains B800 bleaching, and it mostly reflects the B800-to-B850 energy transfer, but likely due to the mixing of various signals, the time constant does not ideally match that obtained from direct B800 excitation. Similar effect was identified earlier (Cong et al. 2008). The final EADS (blue, 1.2 ns) is again the B850 decay. Another, low amplitude component of 16 ps improves the fit, matching the data taken on this LH2 by Cong et al. (Cong et al. 2008) who reported similar component with time constant of 21 ps.

The EADS in the visible region (Fig. 4E) are typical of rhodopin glucoside dynamics in LH2. The initial black EADS due to the S_2 state decays in less than 100 fs to generate EADS (red) of a carotenoid hot S_1 state characterized by increased ESA in the 600–700 nm region. This EADS decays in 0.3 ps to form the relaxed S_1 state of rhodopin glucoside. The S_1 state decays in 3.4 ps, which is close to the lifetime of rhodopin glucoside in solution, confirming the absence of the S_1 -mediated energy transfer pathway. Two other components, 28 (blue) and 300 ps (cyan) are needed to fit the spectral region of carotenoid triplet. Some representative kinetics and fits are shown in Fig. 5.

Fig. 5 **A** Kinetics measured after different excitations at the maximum of the B850 ground state bleaching at 870 nm. **B** The same comparison but for kinetics at the B850 excited state absorption (probe 845 nm). **C** Comparison of kinetics obtained after carotenoid excitation at 525 nm: the S_I-S_N transition at 570 nm (red), S^* signal at 550 nm (black) and B850 ground state bleaching signal at 870 nm (blue, inverted). **D** Kinetics recorded at the maximum of carotenoid triplet (550 nm) after 380 nm (black) and 800 nm (red) excitation. All kinetics were normalized to their maxima



Discussion

The presented data compares excited state dynamics of pigments in LH2 after excitation of either Soret or B800 band of BChl *a*, and the S_2 state of the carotenoid rhodopin glucoside. Even after BChl *a* excitation, the data shows rich, but weak, signals in the spectral region of carotenoid absorption bands, implying the carotenoid response to BChl *a* excitation. Comparison of these data with those obtained after direct carotenoid excitation allows to assess a possible involvement of carotenoid in energy transfer network after BChl *a* excitation. The excited state processes discussed in detail below are summarized in Fig. 6.

Excited state dynamics after Soret excitation

In the near-IR region monitoring the BChl *a* dynamics, excitation of the Soret band generates a typical BChl *a* signal consisting of B850 ESA and GSB, but at earlier times we identify also B800 bleaching. The amplitude of B800 bleaching increases with shifting the excitation wavelength from 380 to 340 nm (Supporting Information, Fig. S2). Thus, the B800 BChl *a* contributes predominantly to the blue part of the Soret band, mirroring the situation of the Q_x band whose blue part is also due to B800 BChl *a* as evidenced from inset of Fig. 3A. The additional fast component required to fit the data obtained after Soret excitation (Fig. 4B) suggests that the Soret band decays to Q_y in less than 200 fs (Fig. 6). The Soret relaxation is even better captured in EADS in Fig. 4A, where the characteristic B800/B850 ESA in 600–700 nm region, which is due to a

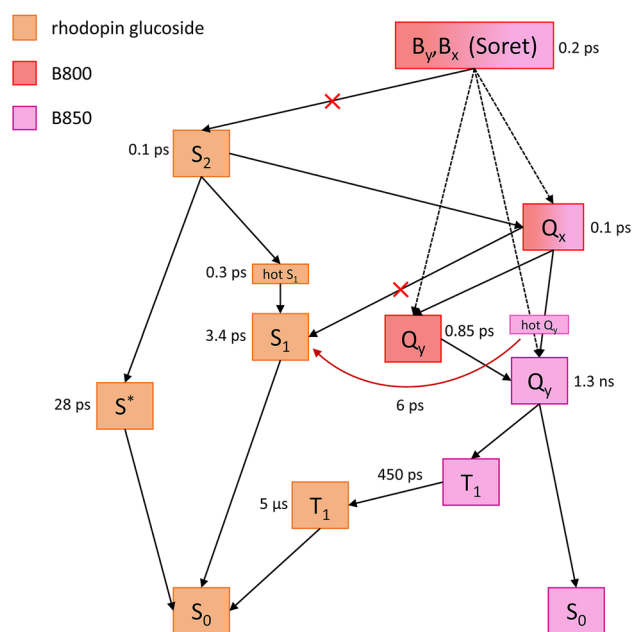


Fig. 6 Model of energy flow in LH2 complex of *Rbl. acidophilus*. Crossed arrows represent predicted energy transfer pathways not confirmed in presented transient absorption measurements. Dashed arrows show BChl *a* Soret-to- Q_y relaxation with a possible involvement of Q_x state. Red arrow represents the rhodopin glucoside response to excess energy dissipation. All numeric values correspond to the lifetimes of individual excited states

transition from the Q_y band, appears with the initial 0.15 ps decay component.

Our data also addresses the question concerning a possible energy transfer channel from the Soret band to the

carotenoid S_2 state. This channel was proposed earlier based on calculations of the Soret- S_2 couplings (Tretiak et al. 2000), but later experimentally challenged by precise measurements of fluorescence excitation spectra of various LH2 complexes (Razjivin et al. 2021, 2017). Here we extend the experimental evaluation of this problem further, confirming that there is indeed no energy transfer from the BChl a Soret band to the S_2 state of rhodopin glucoside in LH2. The data shown in Figs. 2B and 3A unequivocally show that neither carotenoid S_2 - S_N nor S_1 - S_n signal, respectively, is observed after Soret excitation, proving the absence of Soret- S_2 energy transfer.

Since the same conclusion has been reached in other LH2 and LH1 complexes (Razjivin et al. 2017, 2021), it is tempting to conclude that absence of the Soret- S_2 energy transfer is universal among the LH complexes from purple bacteria. As shown by quantum chemical calculations (Razjivin et al. 2021), the main property that prevents the Soret- S_2 energy transfer is unfavorable mutual orientation of the transition dipoles that are nearly orthogonal. Thus, the Soret- S_2 pathway could be in principle opened only in a LH complex having very different mutual orientation of carotenoid and BChl a . A possible candidate could be the heptameric LH2 complex from *Marichromatium purpuratum*, which contains additional carotenoid aligned along the membrane plane (Gardiner et al. 2021), but further experiments and calculations are needed to test this hypothesis.

The absence of any signal related to the carotenoid S_1 state after Soret excitation also confirms we do not excite carotenoid directly at these wavelengths as expected from absorption spectrum of rhodopin glucoside in LH2 (Supporting Information, Fig. S4). Assuming that the Q_x state is populated during the Soret-to- Q_y relaxation, it also implies that there is no Q_x -to- S_1 energy transfer channel either. This pathway was suggested for the RC-LH1 complex from *Rsp. rubrum* that binds the carotenoid spirilloxanthin (Kosumi et al. 2011b), but no evidence for such channel is found in data presented here.

Origin of the carotenoid signal after BChl a excitation

The rich signal in the 450–650 nm spectral region must have its origin in a carotenoid response to BChl a excitation. Since there is no possible pathway that could populate the carotenoid after excitation at 800 nm, the similarity of signals obtained after 380 nm (Soret) and 800 nm (B800) excitations implies they are not due to carotenoid population. Instead, the most likely origin is an electrochromic shift of the carotenoid S_2 state, resulting from a change of local electric field upon BChl a excitation (Gottfried et al. 1991; Herek et al. 1998, 2004).

To verify this assignment, we have followed the approach used by Niedzwiedzki et al. (2016). It is well known that carotenoids bound to LH2 exhibit a bathochromic shift upon excitation of nearby BChl a . The shift in LH2 is much larger than in solvent and this effect has been explained both by the presence of highly polarizable amino acid residues such as arginine in the carotenoid binding site (Herek et al. 2004) and increased local electric field due to the formation of a carotenoid cation (Niedzwiedzki et al. 2016). Following the procedure reported in Niedzwiedzki et al. (2016), we have modeled the expected signal due to electrochromic shift by generating the difference spectrum via subtracting the shifted carotenoid absorption from the ground state absorption spectrum (Fig. 7A). To obtain differential spectrum matching the measured data, bathochromic shift of 940 cm^{-1} is required, which is slightly less than 1000 cm^{-1} reported for LH2 from *Rhodobacter sphaeroides* (Niedzwiedzki et al. 2016).

Figure 7B shows the comparison of the modeled difference spectrum due to electrochromic shift with the measured data at 0.5 and 20 ps delays after 380 nm excitation. Except the BChl a ESA background that is dominant especially

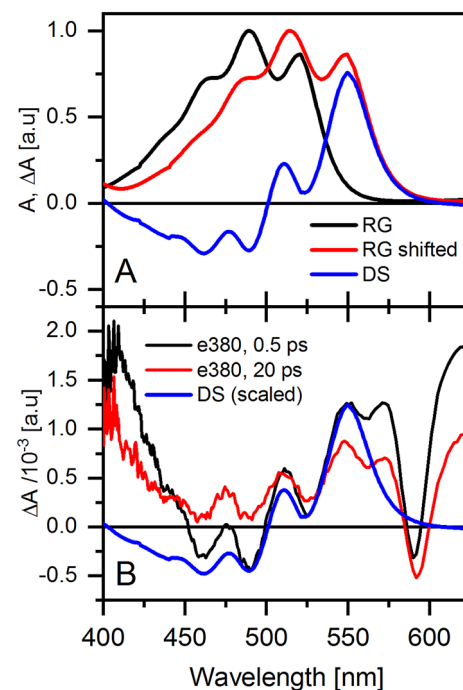


Fig. 7 Modeling of spectral features observed in 450–600 nm region after 380 nm excitation: **A** Expected absorption spectrum of rhodopin glucoside in LH2 complex modeled by absorption spectrum measured in methanol and shifted to match the band position in LH2 (RG, black); the same spectrum but red-shifted by 940 cm^{-1} (RG, red); the corresponding difference spectrum (DS, blue). **B** Comparison of scaled difference spectrum (DS scaled, blue) with the transient absorption spectra measured at 0.5 ps (black) or 20 ps (red) after excitation at 380 nm

below 450 nm and above 570 nm, the agreement is reasonable supporting our assumption that the signal in the carotenoid region after BChl *a* excitation indeed has its origin in electrochromic shift. However, Fig. 3C also shows that if the carotenoid is excited directly, the amplitude of the signal in the 450–570 nm spectral region is much stronger than after BChl *a* excitation. Since the data in Fig. 3C are taken at 20 ps and normalized at B850, the carotenoid response should be comparable for all excitations since at this delay essentially all excitations have reached B850. This is however not the case as direct carotenoid excitation produces a much stronger signal, challenging the assignment of the 550 nm band observed here solely to the electrochromic shift. Instead, this band observed in LH2 after carotenoid excitation has been usually attributed to the carotenoid S^* state (Papagiannakis et al. 2002, 2006) whose origin is still a matter of debate (Balevičius et al. 2016; Hashimoto et al. 2018). Niedzwiedzki et al. (2016) challenged this assignment by an ascription of the 550 nm band to the electrochromic shift, but our data shows that the explanation is likely more complicated.

The stronger signal could have its origin in a stronger local electric field caused by formation of the carotenoid-B800 radical pair, an effect included in the analysis given by Niedzwiedzki et al. (2016). Since the carotenoid-B800 radical pair is observed solely after carotenoid excitation (Polívka et al. 2004), the enhanced signal in Fig. 3C, presumably due to electrochromic shift, could be indeed caused by additional electric field generated by the radical pair that is absent after BChl *a* excitation. However, the efficiency of radical pair generation for LH2 containing rhodopin glucoside is around 10% (Cong et al. 2008), which could hardly explain the approximately fivefold amplification of the signal (Fig. 3C). Our data in the 1000–1100 nm spectral region, where the signal of the rhodopin glucoside radical is expected, also indicates only very weak (if any) contribution of the carotenoid radical (Fig. 3B). Further, the signal at 20 ps delay generated in the 450–510 nm spectral region by carotenoid excitation is negative. This indicates that some carotenoid bleaching most likely contributes, too, because a sole combination of electrochromic shift and BChl *a* background (which is weak, but positive in this spectral region) could hardly produce a purely negative signal. It is thus likely that if the carotenoid is excited, the 550 nm band is combination of electrochromic shift and a signal attributed to the carotenoid S^* state.

Excess energy dissipation

The Soret excitation pumps excess energy of nearly $14,000\text{ cm}^{-1}$ into LH2 compared to the excitation of the B800 band. Since the Soret decay is fast, around 200 fs (Fig. 4B), the extra energy will be stored in vibrations of a

hot excited state of BChl *a*. Further relaxation via internal vibrational redistribution and vibrational cooling associated with vibrational energy transfer to the vibrational modes of the immediate protein environment must occur in the Q_y state, because these processes occur on a time scale of a few picoseconds (Balevičius et al. 2019). Can we see these processes in our data?

In the NIR spectral region, the only difference is extra 0.2 ps component that is clearly associated with the Soret-to- Q_y relaxation and no other time components attributable to excess energy dissipation are identified. In the visible part of the spectrum, however, there is an additional 6.4 ps time component (Fig. 4A) that is needed exclusively to fit the data obtained after 380 nm excitation of the Soret band. Similar component is also needed to fit the data obtained after 340 and 360 nm excitations (Supporting Information, Fig. S5). This component is associated with a decay of the signal due to electrochromic shift (Fig. 4A), suggesting that the extra energy stored in vibrations of excited BChl *a* enhances the electrochromic shift, most likely by slight increase of the local electric field. Thus, while we do not see a clear marker of excess energy stored in vibrations in the BChl *a* signal in NIR, it is sensed by the carotenoid in the vicinity of ‘hot’ excited BChl *a*. The carotenoid in LH2 acts as sensor of excess energy stored in vibrations and the 6.4 ps component associated with decay of the electrochromic shift allows determining the time constant related to excess energy dissipation (Fig. 6).

The 300–600 ps component

There is another time component extracted from global fitting that requires explanation. While the data in the NIR spectral region associated with the BChl *a* signals are readily fitted only with components corresponding to B800–B850 energy transfer and subsequent B850 decay, the visible spectral region requires another component having time constant in the 300–600 ps interval (Fig. 4A, C, E). In contrast to the 6.4 ps component attributed to excess energy dissipation due to excitation of the Soret band, the 300–600 ps component is needed to fit data after Soret, B800 and also rhodopin glucoside excitation, excluding its relation to the excess energy dissipation. Instead, this component has appreciable amplitude only in a narrow spectral interval where the carotenoid triplet appears (Fig. 4A, C, E), pointing to its association with the carotenoid triplet state. Since 450 ps is far too fast for BChl *a* singlet-to-triplet conversion, which would have to be observed also in BChl *a* bleaching decay, but it is not (Fig. 4D), a possibility is that it is a time constant of the BChl *a*-carotenoid triplet–triplet energy transfer (Fig. 6).

To test this hypothesis, we assumed the 0.85 ps, 1.6 ns, and non-decaying EADS obtained from sequential fitting the data in the visible region after B800 excitation (Fig. 4C)

as the difference spectra of the B800, B850, and carotenoid triplet. The only missing species, BChl *a* triplet, was simulated by a scaled B850 spectrum, since the BChl *a* triplet in solution has a difference spectrum comparable to the B850 Q_y state (Niedziedzki and Blankenship 2010). Using this approximation, we used these modeled ‘species associated difference spectra’ to generate kinetics of triplet rise under conditions of ‘reverse’ kinetic scheme with B850 singlet–triplet conversion of 1.6 ns and 450 ps triplet–triplet energy transfer (the second process is faster than the first one). The resulting kinetic is, along with the measured data, shown in Supporting Information, Fig. S6. Although the match is not ideal, it is obvious that even under this approximation we can qualitatively reproduce the data, especially the shape of the kinetic featuring a 450 ps decay and 1.6 ns rise. The ‘reverse’ kinetic scheme causes the 450 ps component appearing as a decay and it also explains why the BChl *a* triplet is not detectable in the data; due to the reverse kinetic scheme the BChl *a* triplet population is extremely small, preventing its detection in data. Although such triplet dynamics has not been considered for LH2 (Kosumi et al. 2016), we note that similar scheme was identified in LHCII, where the Chl *a*-to-carotenoid triplet–triplet transfer was 500 ps, much faster than the Chl *a* singlet–triplet conversion (Schödel et al. 1998). Even faster Chl-carotenoid triplet–triplet transfer of about 100 ps was estimated in antenna complexes from dinoflagellates (Kvíčalová et al. 2016). Our data show that comparable triplet dynamics occurs also in LH2, suggesting that kinetic scheme featuring (B)Chl-carotenoid triplet–triplet energy transfer faster than (B)Chl singlet–triplet conversion is likely common in photosynthetic antenna systems.

Conclusion

We have exposed the LH2 complex from *Rbl. acidophilus* to excess energy excitation by exciting the Soret band of BChl *a*. Our ultrafast transient absorption data show that there is no energy transfer between the Soret band and the S_2 state of carotenoid. The Soret band of BChl *a* decays to the Q_y state within less than 200 fs. The excess energy is stored in vibrational modes of the Q_y state that is hot after internal conversion from the Soret band. The carotenoid nearby responds to the excess of vibrational energy in the Q_y state, resulting in increased amplitude of the signal associated with electrochromic shift of the carotenoid S_2 state. The carotenoid response to excess energy dissipation in excited BChl *a* indicates the cooling of the BChl *a* Q_y state. Global analysis and following reverse modeling of transient absorption data in the visible spectral region have also allowed to identify a sub-nanosecond triplet–triplet energy transfer between BChl *a* and carotenoid rhodopin glucoside. The

triplet–triplet energy transfer is faster than singlet–triplet intersystem crossing, supporting a kinetic scheme known from light-harvesting complexes from other photosynthetic organisms.

Supplementary Information The online version contains supplementary material available at <https://doi.org/10.1007/s1120-022-00952-5>.

Funding Funding was provided from the Czech Science Foundation, Grant No. 19-28323X.

Declarations

Conflict of interest The authors declare that they have no conflict of interest.

References

- Balevičius V, Abramavicius D, Polívka T et al (2016) A unified picture of S_2 in carotenoids. *J Phys Chem Lett* 7:3347–3352. <https://doi.org/10.1021/acs.jpcllett.6b01455>
- Balevičius V, Wei T, Di Tommaso D et al (2019) The full dynamics of energy relaxation in large organic molecules: from photo-excitation to solvent heating. *Chem Sci* 10:4792–4804. <https://doi.org/10.1039/c9sc00410f>
- Billsten HH, Pan J, Sinha S et al (2005) Excited-state processes in the carotenoid zeaxanthin after excess energy excitation. *J Phys Chem A* 109:6852–6859. <https://doi.org/10.1021/jp052227s>
- Blankenship RE (2008) *Molecular mechanisms of photosynthesis*. Wiley, Hoboken
- Bricker WP, Shenai PM, Ghosh A et al (2015) Non-radiative relaxation of photoexcited chlorophylls: theoretical and experimental study. *Sci Rep* 5:1–16. <https://doi.org/10.1038/srep13625>
- Cong H, Niedziedzki DM, Gibson GN et al (2008) Ultrafast time-resolved carotenoid to-bacteriochlorophyll energy transfer in LH2 complexes from photosynthetic bacteria. *J Phys Chem B* 112:10689–10703. <https://doi.org/10.1021/jp711946w>
- Croce R, Van Amerongen H (2014) Natural strategies for photosynthetic light harvesting. *Nat Chem Biol* 10:492–501. <https://doi.org/10.1038/nchembio.1555>
- Croce R, Müller MG, Bassi R, Holzwarth AR (2001) Carotenoid-to-chlorophyll energy transfer in recombinant major light-harvesting complex (LHCII) of higher plants. I. Femtosecond transient absorbance measurements. *Biophys J* 80:901–915. [https://doi.org/10.1016/S0006-3495\(01\)76069-9](https://doi.org/10.1016/S0006-3495(01)76069-9)
- Ferrante C, Pontecorvo E, Cerullo G et al (2016) Direct observation of subpicosecond vibrational dynamics in photoexcited myoglobin. *Nat Chem* 8:1137–1143. <https://doi.org/10.1038/nchem.2569>
- Gardiner AT, Naydenova K, Castro-Hartmann P et al (2021) The 2.4 Å cryo-EM structure of a heptameric light-harvesting 2 complex reveals two carotenoid energy transfer pathways. *Sci Adv*. <https://doi.org/10.1126/sciadv.abe4650>
- Gottfried DS, Steffen MA, Boxer SG (1991) Large protein-induced dipoles for a symmetric carotenoid in a photosynthetic antenna complex. *Science* 251:662–665. <https://doi.org/10.1126/science.1992518>
- Gradinaru CC, Kennis JTM, Papagiannakis E et al (2001) An unusual pathway of excitation energy deactivation in carotenoids: singlet-to-triplet conversion on an ultrafast timescale in a photosynthetic antenna. *Proc Natl Acad Sci USA* 98:2364–2369. <https://doi.org/10.1073/pnas.051501298>

- Hashimoto H, Uragami C, Yukihiro N et al (2018) Understanding/unravelling carotenoid excited singlet states. *J R Soc Interface*. <https://doi.org/10.1098/rsif.2018.0026>
- Herek JL, Polívka T, Pullerits T et al (1998) Ultrafast carotenoid band shifts probe structure and dynamics in photosynthetic antenna complexes. *Biochemistry* 37:7057–7061. <https://doi.org/10.1021/bi980118g>
- Herek JL, Wendling M, He Z et al (2004) Ultrafast carotenoid band shifts: experiment and theory. *J Phys Chem B* 108:10398–10403. <https://doi.org/10.1021/jp040094p>
- Jailaubekov AE, Song SH, Vengris M et al (2010) Using narrow-band excitation to confirm that the S* state in carotenoids is not a vibrationally-excited ground state species. *Chem Phys Lett* 487:101–107. <https://doi.org/10.1016/j.cplett.2010.01.014>
- Kennis JTM, Streltsov AM, Vulto SIE et al (1997) Femtosecond dynamics in isolated LH2 complexes of various species of purple bacteria. *J Phys Chem B* 101:7827–7834. <https://doi.org/10.1021/jp963359b>
- Khan T, Litvín R, Šebelík V, Polívka T (2021) Excited-state evolution of keto-carotenoids after excess energy excitation in the UV region. *Chem Phys Chem* 22:471–480. <https://doi.org/10.1002/cphc.202000982>
- Kholodenko Y, Volk M, Gooding E, Hochstrasser RM (2000) Energy dissipation and relaxation processes in deoxy myoglobin after photoexcitation in the solet region. *Chem Phys* 259:71–87. [https://doi.org/10.1016/S0301-0104\(00\)00182-8](https://doi.org/10.1016/S0301-0104(00)00182-8)
- Konold PE, Van Stokkum IHM, Muzzopappa F et al (2019) Photoactivation mechanism, timing of protein secondary structure dynamics and carotenoid translocation in the orange carotenoid protein. *J Am Chem Soc* 141:520–530. <https://doi.org/10.1021/jacs.8b11373>
- Koolhaas MHC, Frese RN, Fowler GJS et al (1998) Identification of the upper exciton component of the b850 bacteriochlorophylls of the LH2 antenna complex, using a B800-free mutant of *Rhodospira sphaeroides*. *Biochemistry* 37:4693–4698. <https://doi.org/10.1021/bi9730361>
- Kosumi D, Maruta S, Fujii R et al (2011a) Ultrafast excited state dynamics of monomeric bacteriochlorophyll a. *Phys Status Solidi C* 8:92–95. <https://doi.org/10.1002/pssc.201000684>
- Kosumi D, Maruta S, Horibe T et al (2011b) Ultrafast energy-transfer pathway in a purple-bacterial photosynthetic core antenna, as revealed by femtosecond time-resolved spectroscopy. *Angew Chem Int Ed* 50:1097–1100. <https://doi.org/10.1002/anie.201003771>
- Kosumi D, Nakagawa K, Sakai S et al (2013) Ultrafast intramolecular relaxation dynamics of Mg- and Zn-bacteriochlorophyll a. *J Chem Phys* 139:1–8. <https://doi.org/10.1063/1.4813526>
- Kosumi D, Horibe T, Sugisaki M et al (2016) Photoprotection mechanism of light-harvesting antenna complex from purple bacteria. *J Phys Chem B* 120:951–956. <https://doi.org/10.1021/acs.jpcc.6b00121>
- Kvíčalová Z, Alster J, Hofmann E et al (2016) Triplet-triplet energy transfer from chlorophylls to carotenoids in two antenna complexes from dinoflagellate *Amphidinium carterae*. *Biochim Biophys Acta* 1857:341–349. <https://doi.org/10.1016/j.bbabi.2016.01.008>
- Lenzer T, Ehlers F, Scholz M et al (2010) Assignment of carotene S* state features to the vibrationally hot ground electronic state. *Phys Chem Chem Phys* 12:8832–8839. <https://doi.org/10.1039/b925071a>
- Levantino M, Schirò G, Lemke HT et al (2015) Ultrafast myoglobin structural dynamics observed with an X-ray free-electron laser. *Nat Commun* 6:1–6. <https://doi.org/10.1038/ncomms7772>
- Ma YZ, Cogdell RJ, Gillbro T (1997) Energy transfer and excitation annihilation in the B800–850 antenna complex of the photosynthetic purple bacterium *Rhodospseudomonas acidophila* (strain 10050). A femtosecond transient absorption study. *J Phys Chem B* 101:1087–1095. <https://doi.org/10.1021/jp962470e>
- Macpherson AN, Arellano JB, Fraser NJ et al (2001) Efficient energy transfer from the carotenoid S2 state in a photosynthetic light-harvesting complex. *Biophys J* 80:923–930. [https://doi.org/10.1016/S0006-3495\(01\)76071-7](https://doi.org/10.1016/S0006-3495(01)76071-7)
- Magdaong NM, Lafountain AM, Greco JA et al (2014) High efficiency light harvesting by carotenoids in the LH2 complex from photosynthetic bacteria: Unique adaptation to growth under low-light conditions. *J Phys Chem B* 118:11172–11189. <https://doi.org/10.1021/jp5070984>
- McDermott G, Prince SM, Freer AA et al (1995) Crystal structure of an integral membrane light-harvesting complex from photosynthetic bacteria. *Nature* 374:517–521
- Mirkovic T, Ostroumov EE, Anna JM et al (2017) Light absorption and energy transfer in the antenna complexes of photosynthetic organisms. *Chem Rev* 117:249–293. <https://doi.org/10.1021/acs.chemrev.6b00002>
- Niedzwiedzki DM, Blankenship RE (2010) Singlet and triplet excited state properties of natural chlorophylls and bacteriochlorophylls. *Photosynth Res* 106:227–238. <https://doi.org/10.1007/s11120-010-9598-9>
- Niedzwiedzki DM, Hunter CN, Blankenship RE (2016) Evaluating the nature of so-called S*-state feature in transient absorption of carotenoids in light-harvesting complex 2 (LH2) from purple photosynthetic bacteria. *J Phys Chem B* 120:11123–11131. <https://doi.org/10.1021/acs.jpcc.6b08639>
- Papagiannakis E, Kennis JTM, Van Stokkum IHM et al (2002) An alternative carotenoid-to-bacteriochlorophyll energy transfer pathway in photosynthetic light harvesting. *Proc Natl Acad Sci USA* 99:6017–6022. <https://doi.org/10.1073/pnas.092626599>
- Papagiannakis E, Van Stokkum IHM, Vengris M et al (2006) Excited-state dynamics of carotenoids in light-harvesting complexes. 1. Exploring the relationship between the S1 and S* states. *J Phys Chem B* 110:5727–5736. <https://doi.org/10.1021/jp054633h>
- Polívka T, Frank HA (2010) Molecular factors controlling photosynthetic light harvesting by carotenoids. *Acc Chem Res* 43:1125–1134. <https://doi.org/10.1021/ar100030m>
- Polívka T, Sundström V (2004) Ultrafast dynamics of carotenoid excited states—from solution to natural and artificial systems. *Chem Rev* 104:2021–2071. <https://doi.org/10.1021/cr020674n>
- Polívka T, Pullerits T, Frank HA et al (2004) Ultrafast formation of a carotenoid radical in LH2 antenna complexes of purple bacteria. *J Phys Chem B* 108:15398–15407. <https://doi.org/10.1021/jp0483019>
- Razjivin AP, Lukashev EP, Kompanets VO et al (2017) Excitation energy transfer from the bacteriochlorophyll solet band to carotenoids in the LH2 light-harvesting complex from *Ectothiorhodospira haloalkaliphila* is negligible. *Photosynth Res* 133:289–295. <https://doi.org/10.1007/s11120-017-0341-7>
- Razjivin A, Götte J, Lukashev E et al (2021) Lack of excitation energy transfer from the bacteriochlorophyll solet band to carotenoids in photosynthetic complexes of purple bacteria. *J Phys Chem B* 125:3538–3545. <https://doi.org/10.1021/acs.jpcc.1c00719>
- Schödel R, Irrgang KD, Voigt J, Renger G (1998) Rate of carotenoid triplet formation in solubilized light-harvesting complex II (LHCII) from spinach. *Biophys J* 75:3143–3153. [https://doi.org/10.1016/S0006-3495\(98\)77756-2](https://doi.org/10.1016/S0006-3495(98)77756-2)
- Shi Y, Liu JY, Han KL (2005) Investigation of the internal conversion time of the chlorophyll a from S3, S2 to S1. *Chem Phys Lett* 410:260–263. <https://doi.org/10.1016/j.cplett.2005.05.017>

- Sundström V, Pullerits T, Van Grondelle R (1999) Photosynthetic light-harvesting: reconciling dynamics and structure of purple bacterial LH2 reveals function of photosynthetic unit. *J Phys Chem B* 103:2327–2346. <https://doi.org/10.1021/jp983722+>
- Tretiak S, Middleton C, Chernyak V, Mukamel S (2000) Bacteriochlorophyll and carotenoid excitonic couplings in the LH2 system of purple bacteria. *J Phys Chem B* 104:9540–9553. <https://doi.org/10.1021/jp001585m>
- Visser HM, Somsen OJ, van Mourik F et al (1995) Direct observation of sub-picosecond equilibration of excitation energy in the light-harvesting antenna of *Rhodospirillum rubrum*. *Biophys J* 69:1083–1099. [https://doi.org/10.1016/S0006-3495\(95\)79982-9](https://doi.org/10.1016/S0006-3495(95)79982-9)
- Zang C, Stevens JA, Link JJ et al (2009) Ultrafast proteinquake dynamics in cytochrome c. *J Am Chem Soc* 131:2846–2852. <https://doi.org/10.1021/ja8057293>

Publisher's Note Springer Nature remains neutral with regard to jurisdictional claims in published maps and institutional affiliations.

Springer Nature or its licensor holds exclusive rights to this article under a publishing agreement with the author(s) or other rightsholder(s); author self-archiving of the accepted manuscript version of this article is solely governed by the terms of such publishing agreement and applicable law.